



Contents lists available at SciVerse ScienceDirect

Sensors and Actuators B: Chemical

journal homepage: www.elsevier.com/locate/snb



UV-assisted alcohol sensing using SnO₂ functionalized GaN nanowire devices

Ritu Bajpai^{a,b}, Abhishek Motayed^{b,c,*}, Albert V. Davydov^b, Vladimir P. Oleshko^b, Geetha S. Aluri^{b,d}, Kris A. Bertness^e, Mulpuri V. Rao^d, Mona E. Zaghloul^a

^a Department of Electrical and Computer Engineering, The George Washington University, Washington, DC 20052, USA

^b Material Measurement Laboratory, National Institute of Standards and Technology (NIST), Gaithersburg, MD 20899, USA

^c Institute for Research in Electronics and Applied Physics, University of Maryland, College Park, MD 20742, USA

^d Department of Electrical and Computer Engineering, George Mason University, Fairfax, VA 22030, USA

^e Physical Measurement Laboratory, National Institute of Standards and Technology, Boulder, CO 80305, USA

ARTICLE INFO

Article history:

Received 22 December 2011

Received in revised form 1 May 2012

Accepted 4 May 2012

Available online xxx

Keywords:

Alcohol sensor

GaN nanowire

Photoconductivity

Semiconducting metal oxide

ABSTRACT

A chemiresistor type sensor for selective alcohol sensing has been realized from gallium nitride (GaN) nanowires (NWs) functionalized with sputter-deposited tin dioxide (SnO₂) nanoparticles. Two-terminal devices were fabricated using standard microfabrication techniques with the individual NWs air-bridged between the two metal contact pads. Through a combination of X-ray diffraction (XRD), electron-backscatter-diffraction (EBSD), and TEM/STEM techniques, we confirmed the presence of rutile SnO₂ nanocrystals on the GaN surface. A change in device current is observed when the device is exposed to alcohol vapors (methanol, ethanol, propanol, and butanol) at room temperature under 215–400 nm UV illumination with 3.75 mW/m² intensity at 365 nm wavelength. The sensor reproducibly responded to a wide range of alcohol vapor concentrations, from 5000 μmol/mol (ppm) down to 1 μmol/mol (ppm) in air. Notably, the devices show low sensitivity to acetone and hexane, which allows them to selectively detect the primary alcohol vapors mixed with these two common volatile organic compounds (VOCs). The sensor response was not observed without UV excitation. From the experimental results we found a relationship between the response towards the alcohol vapors and the length of carbon chain in the molecule: the chemiresistive response decreases with the increasing carbon chain from methanol to n-butanol. In addition, we observed that the isomeric branching in i-propanol and i-butanol caused reduced response as compared to n-propanol and n-butanol, respectively. We have qualitatively explained the sensor operation by employing a mechanism, which includes oxidation of analyte molecules on the SnO₂ surface, leading to enhanced photoconductivity in GaN nanowire.

© 2012 Elsevier B.V. All rights reserved.

1. Introduction

Solid state chemiresistor-type gas sensors are popular alternatives to traditional devices based on chromatography, nuclear magnetic resonance (NMR), and mass spectroscopy due to miniaturization, portability, reduced power consumption, high sensitivity, quick response, and fast refresh rate [1]. Semiconducting metal oxides thin films are used for gas sensing [1,2] because their transport properties readily respond to the adsorbed analytes. Recently, nanowires and other nano-structures of these materials have been shown to exhibit even better sensing characteristics due to increased surface area, reduction in size and power consumption, and nmol/mol (ppb) sensitivity [3,4].

Chemical dopants [5] and catalytic additives [6] have been introduced to nanowires to enhance their selectivity and efficiency. In other cases, surface nanoclusters and nanoparticles have been used as transducers for the chemically inert nanowires. For example, it has been shown that GaN NWs can be surface functionalized to induce sensitivity towards specific analytes [7–9]. These sensors provide the flexibility to start with an analyte-inert nanowire material and make them selectively sensitive based on the surface functionalization. In this paper we have presented SnO₂-coated GaN nanowires for selective alcohol sensing. SnO₂ is one of the most widely used metal oxide for gas sensing [10–12]. Surface properties of SnO₂ make it a popular candidate for fabricating thin films [13], nanoparticle arrays [14,15], NWs, and other nanostructured gas sensors [16–20]. Additionally, photoconductive properties of SnO₂ have been used for making photodetectors and other devices [21–23]. Closely matching band gap (GaN 3.4 eV and SnO₂ 3.65 eV [24]) and photoconductive properties of GaN and SnO₂, combined with surface properties of SnO₂, make them suitable candidates for fabricating the GaN NW/SnO₂ nanocluster hybrid sensors described in this paper.

* Corresponding author at: Institute for Research in Electronics and Applied Physics, University of Maryland, College Park, MD 20742, USA. Tel.: +1 301 975 6159; fax: +1 301 975 4553.

E-mail address: amotayed@nist.gov (A. Motayed).

We have used the change in photoconductivity of the hybrid SnO_2 -nanocrystals/GaN-NW devices when exposed to analytes as a sensing parameter. The rapid photoresponse of the nanostructures and NWs compared to thin films can enhance the sensitivity and reduce the recovery time of the sensor. Photoassisted sensing enables sensors to operate at room temperature in contrast to industrial metal oxide sensors that operate at elevated temperature. Useful properties of photoassisted sensors, such as fast and enhanced gas response have been demonstrated earlier [25–27]. It has also been shown that the device sensitivity can be modulated by varying the intensity of light [28]. Along with repeatable and quick response, SnO_2 /GaN hybrid sensors give us a selective response towards alcohols that fall into the category of VOC industrial pollutants.

2. Experiment

2.1. Device fabrication

Si doped, *c*-axis, *n*-type GaN nanowires were grown using catalyst free molecular beam epitaxy on Si (1 1 1) substrates. The NWs were 21–23 μm long and had hexagonal cross-sections of 250–350 nm in diameter. The details of nanowire growth can be found elsewhere [29,30]. The NWs were removed from the silicon substrate by sonication in isopropanol. The device fabrication steps are summarized in Fig. 1. Alignment electrodes were pre-fabricated on sapphire substrate using photolithography followed by deposition of titanium (40 nm)/aluminum (420 nm)/titanium (40 nm) metal stack. The NWs were suspended across these electrodes using dielectrophoretic alignment. The top contacts to the NW ends were formed by depositing titanium (70 nm)/aluminum (70 nm)/titanium (40 nm)/gold (40 nm) multilayer [31].

These two-terminal, freely suspended NW devices were functionalized for gas sensing by RF sputtering of tin dioxide nanocrystals on the NW surface. The SnO_2 target was sputtered with an RF power of 200 W in 30 sccm (standard cubic centimeter) of oxygen and 20 sccm of argon gas flow, while sample temperature was held at 90 °C. It was found that 7 min deposition time was optimal for the formation of uncoalesced oxide nanocrystals on the nanowire surface.

A rapid thermal anneal (RTA) was performed on these devices at 700 °C for 30 s under a 6000 sccm flow of ultra-high purity Ar to facilitate ohmic contact formation to NWs. RTA optimized the device in three ways: (i) it facilitated ohmic contact formation to NWs, (ii) it induced recrystallization of the SnO_2 nanoclusters, and (iii) it reduced mechanical stresses in the thick alignment electrode metal stack of Ti (40 nm)/Al (420 nm)/Ti (40 nm), which is an important consideration for wire bonding the devices. Bond pads were fabricated in the final photolithography step with the deposition of another metal stack of Ti (40 nm)/Au (120 nm). The device was then mounted on a 24-pin ceramic package and the wire bonds were established.

2.2. Device microstructure characterization

The microstructure and morphology of the hybrid SnO_2 -nanoclusters/GaN-NW structures was characterized by field-emission scanning electron microscopy (FESEM), high-resolution analytical transmission and scanning transmission electron microscopy (HR-ATEM/STEM), and selected-area electron diffraction (SAED). The specimens were analyzed in a FEI Titan

80–300 TEM/STEM¹ microscope operating at 300 kV accelerating voltage. The instrument was also equipped with an EDAX Si/Li energy-dispersive X-ray spectrometer and high-angle annular dark-field (HAADF), bright-field (BF), and ADF STEM detectors to perform spot, line profile and areal compositional analyses.

The identification of crystalline phases was also performed by X-ray diffraction (XRD) and electron-backscatter-diffraction (EBSD). The XRD spectra were collected using a Bruker-AXS D8 scanning X-ray micro-diffractometer equipped with a general area detector diffraction system (GADDS) using $\text{Cu-K}\alpha$ radiation. The EBSD patterns were recorded using an HKL Nordlys II EBSD detector attached to the Hitachi S-4700 FESEM.

2.3. Measurement setup

For the gas sensing measurements the device was placed in a custom-made stainless steel chamber with a volume of 0.73 cm^3 and a top quartz window. The device measurements were performed using an Agilent B1500A semiconductor parameter analyzer. A 25 W deuterium bulb (DH-2000-BAL, Ocean Optics) was connected to a fiber optic cable, 600 μm in diameter, which terminated with a collimating lens. This set-up provided uniform intensity over the entire sample surface. The wavelength of the light bulb is confined to the range of 215–400 nm and the intensity recorded was 3.75 nW/cm^2 at 365 nm wavelength. Compressed, “breathing” quality air (<9 ppm of water) was used as the carrier gas in all the sensing measurements and the net flow (air + analyte vapors) was maintained at 40 sccm. All sensing measurements were performed at room temperature, under a DC bias voltage of 5 V.

3. Results

3.1. Microstructural and electrical properties

Fig. 2a shows FESEM image of a typical device with a SnO_2 coated GaN nanowire suspended between the two metal electrodes. Fig. 2b shows the dark current–voltage (*I*–*V*) characteristic of the device, which has an ohmic behavior.

The individual NW devices were too small to obtain XRD from the tin oxide nanocrystals, therefore a reference sample with the tin oxide film on GaN/sapphire substrate was prepared. SnO_2 was sputtered for 1 h to form a 40 nm thick film followed by RTA for 30 s at 700 °C with the assumption that the oxide would have crystallinity similar to the device structures that were annealed under the same conditions. XRD results in Fig. 3 indicate that SnO_2 film is polycrystalline with the rutile structure. These results were supported by EBSD analysis. Fig. 4c and d shows EBSD from individual SnO_2 clusters on GaN NWs, for oxide deposition time of 15 min followed by RTA at 700 °C for 30 s.

Further investigation on the SnO_2 nanoparticles on the GaN NWs was performed using HR-ATEM/STEM techniques. For this purpose, SnO_2 was sputter deposited on an array of vertically standing GaN NWs on a silicon substrate, followed by RTA at 700 °C for 30 s to replicate the thermal processing of the device fabrication steps. Finally, the oxide coated NWs were transferred onto a TEM grid. Fig. 5 presents a HRTEM micrograph of a GaN NW fragment decorated with randomly distributed partially coalesced 5–10 nm tin oxide nanoclusters. As one can see from the figure, the particles exhibit crystallinity. The FFT pattern from the red square in upper

¹ Commercial equipment and material suppliers are identified in this paper to adequately describe experimental procedures. This does not imply endorsement by NIST.

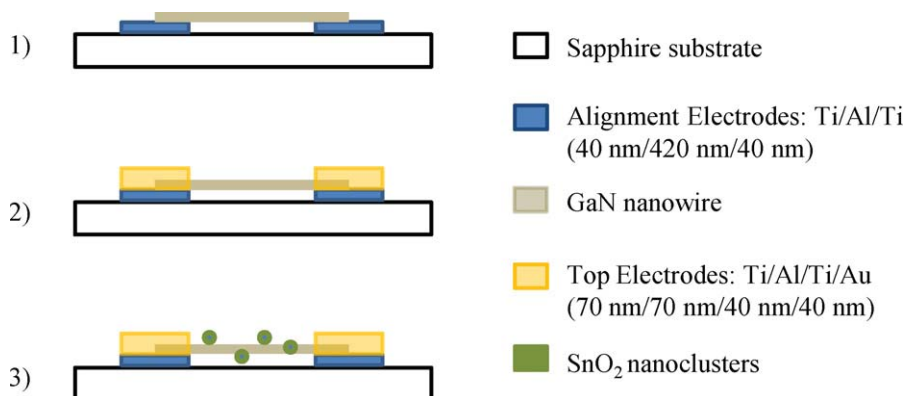


Fig. 1. Fabrication steps for the SnO₂ nanocluster coated GaN nanowire alcohol sensor.

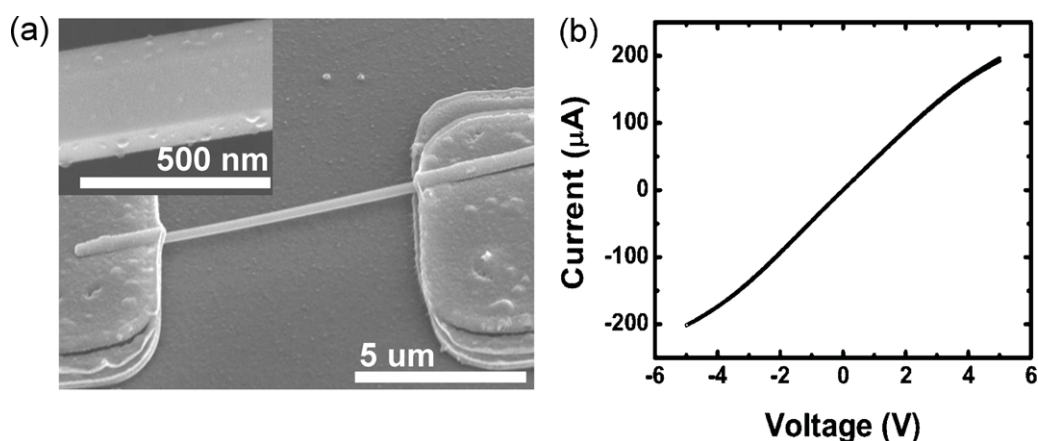


Fig. 2. (a) FESEM image of a GaN suspended bridge structure. Inset shows nanowire facets with tin oxide nanoclusters (b) dark I - V characteristic of the GaN nanowire sensor coated with SnO₂ nanocrystals after RTA at 700 °C for 30 s in argon.

right inset indicates 0.34 nm lattice fringes, which are consistent with a (1 1 0) reflecting plane of the tetragonal polymorph of SnO₂.

Simultaneous BF- and HAADF- (Z-contrast) STEM imaging was employed to enhance visualization of SnO₂ nanoparticles often barely visible against the much thicker GaN NWs. Complementary BF- and HAADF-STEM images of a tip of a GaN NW coated with SnO₂ are shown in Fig. 6a and b respectively. SnO₂ nanoparticles, dark in (a) and bright in (b) STEM images were found to decorate facets of the nanowire and often form elongated aggregates involving several smaller clusters. Fig. 6c presents a spot X-ray spectrum of an individual nanocluster acquired at the nanowire surface (see

right inset), revealing the Sn K α ₁ line at 25.27 keV, the Sn K β ₁ line at 28.48 keV, and the Sn L-series between 3.04 keV and 4.46 keV together with the O K line at 0.52 keV. The Ga K α ₁ line at 9.25 keV, the Ga K β ₁ line at 10.26 keV, and the Ga L-series between 0.96 keV and 1.30 keV were also observed. However, nitrogen (the N K α line at 0.39 keV) was not detected in this particular case. The C K α ₁ line at 0.28 keV, the Cu K α ₁ line at 8.05 keV and the Cu K β ₁ at 8.90 keV belong to materials of the supporting TEM grid.

3.2. Sensor test results

To establish the sensor baseline, a bare GaN NW device was tested at room temperature for response to UV light and other chemical vapors. Increase and decrease in the device current was observed when the UV light was turned on and off respectively. Notably, the device did not respond to any chemical vapors in the presence of UV light. However, when a SnO₂ functionalized NW device was tested at room temperature, a change in the device photocurrent was observed when the chamber was flushed with breathing air (with or without organic vapors) in the presence of UV light. Since compressed breathing air was used as a carrier gas in analyte sensing experiments, the device current recorded with 40 sccm of air flowing through the sensing chamber under UV illumination was established as a reference for our experiments.

Fig. 7a shows the response of the sensor to 500 μ mol/mol (ppm) of methanol, ethanol, n-propanol and n-butanol. During the sensing process, the flow of analyte mixed in breathing air is 40 sccm which is turned on and off for a period of 300 s each. Two sets of readings were recorded for each analyte concentration. The first reading was

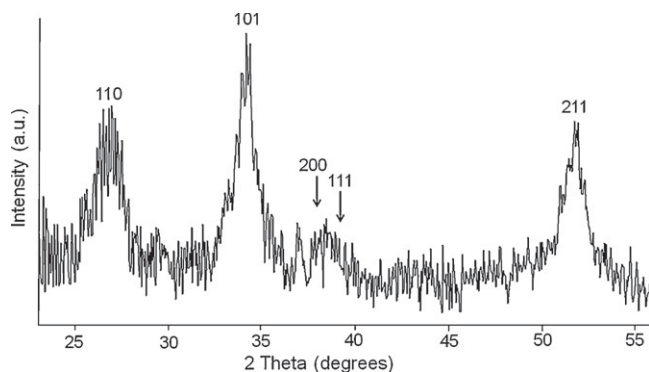


Fig. 3. XRD Ω - 2Θ scan of a 40 nm thick SnO₂ film after 700 °C anneal in argon for 30 s. Indices correspond to tetragonal SnO₂ phase (P42/mnm) with $a = 4.758(3)$ Å and $c = 3.175(2)$ Å lattice parameters.

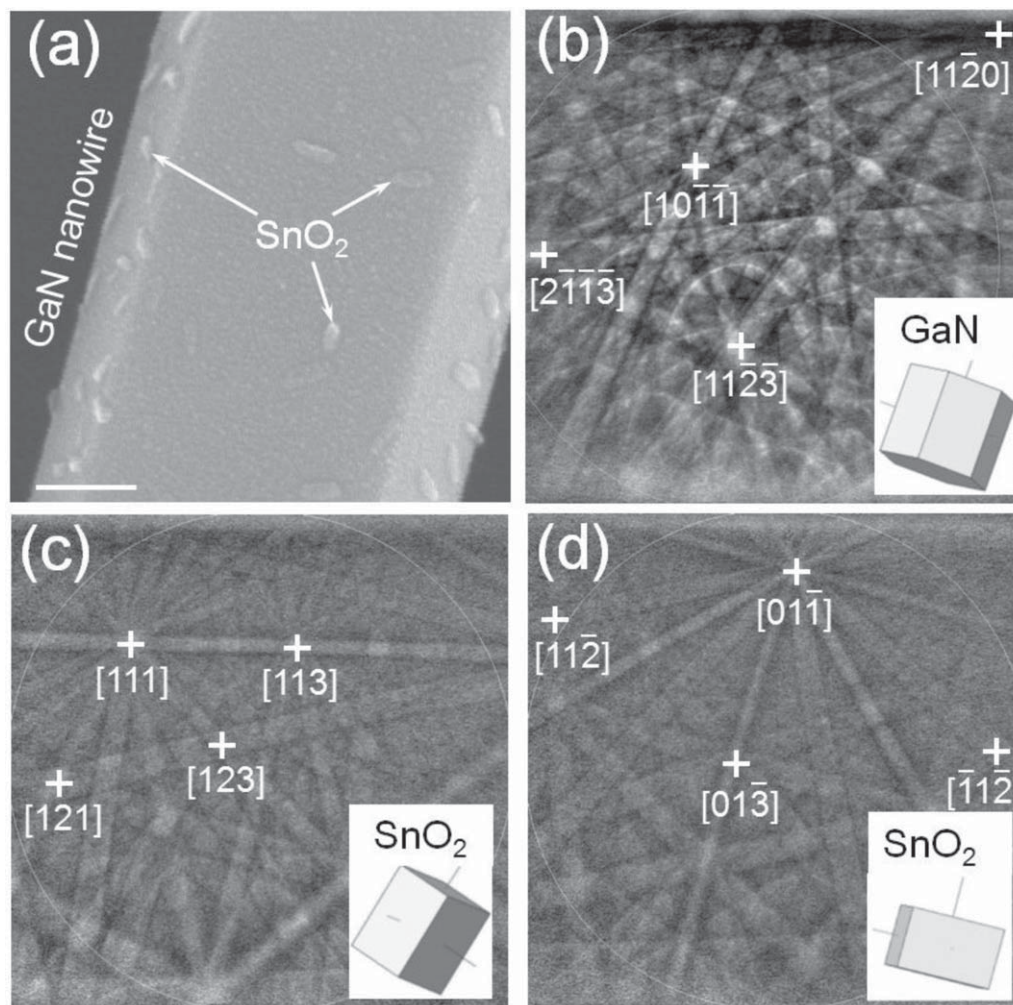


Fig. 4. FESEM image of the nanowire fragment decorated with tin oxide nanoparticles (a); EBSD patterns of GaN (b) and SnO₂ (c–d) with simulated unit cells in the insets. Unit cells in (c) and (d) indicate random crystallographic orientation of SnO₂ grains on GaN surface. Scale bar in (a) is 100 nm.

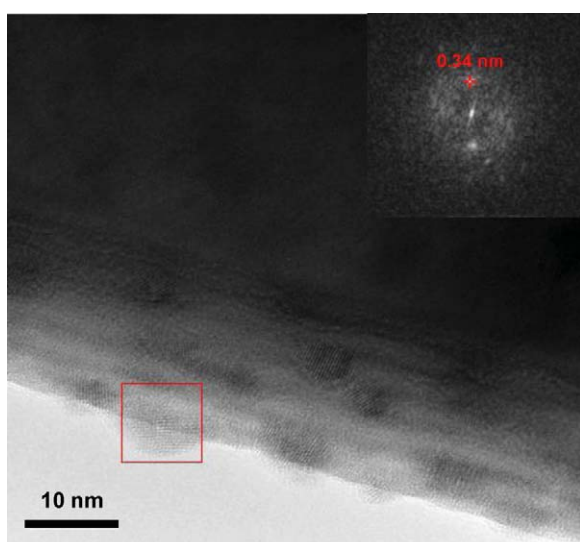


Fig. 5. HRTEM image of a nanowire fragment decorated with randomly distributed 5–10 nm tin oxide nanoclusters, FFT pattern from the red square in upper right inset indicates 0.34 nm lattice fringes, which are consistent with a (1 1 0) reflecting plane of the tetragonal polymorph of SnO₂. (For interpretation of the references to color in this figure legend, the reader is referred to the web version of the article.)

not included in the reported results, it was for gas flow stabilization and ensuring that any residuals of the previously tested chemicals were flushed out. The successive measurement of the same analyte concentration was recorded as the valid data. After analyte testing, once the flow of active component in the gas mixture is off, the sensor recovers to the near initial value of the current.

As it can be seen from Fig. 7a, all alcohols induce current increase relative to the reference, with the highest response being to methanol at fixed concentration of the analytes. As expected, photocurrent increases with increasing concentration of analyte (see Fig. 7b for the methanol case).

The behavior of the device towards water was similar to the behavior towards alcohols, i.e., an increase in photoconductivity was observed with increasing concentration of water vapors as shown in Fig. 7c. The photocurrent baseline in breathing air flow in Fig. 7c likely carries a “history” of water molecules pre-adsorbed on the NW surfaces [32].

Fig. 7d shows the response of the device to 40 sccm of N₂ flow through the chamber. An increase in device current is seen when N₂ gas is flushed through the chamber in the presence of UV light. However when other chemical vapors including alcohol vapors are passed through the chamber mixed in N₂ gas in the presence of light, no further change in device response is observed. Consistent with other chemicals tested, no change in conductivity was observed in dark when nitrogen gas flow was turned on and off into the chamber.

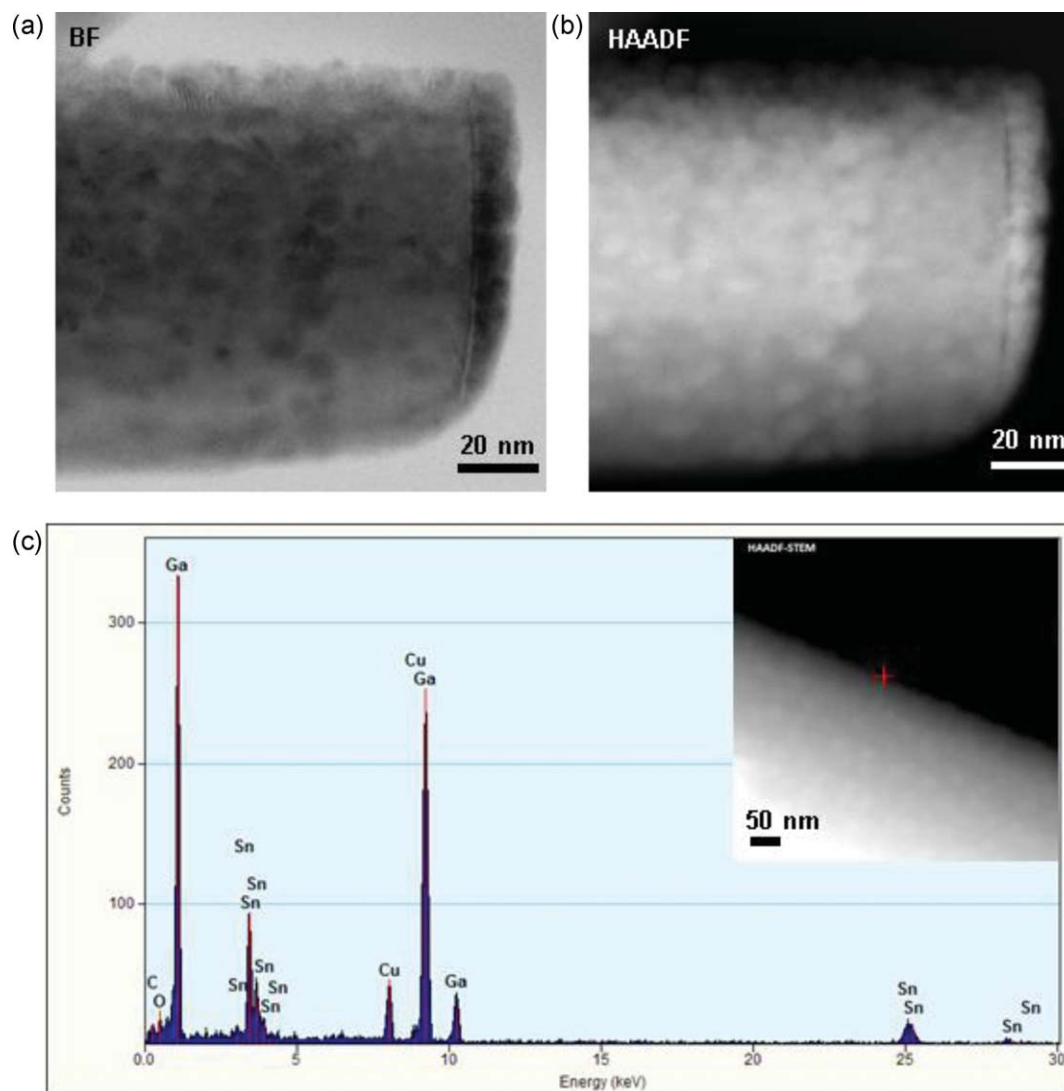


Fig. 6. (a) BF-STEM image of a tip of a GaN nanowire coated with 5–10 nm diameter SnO₂ nanoclusters forming densely packed chain-like aggregates. (b) HAADF-STEM image of the same area. SnO₂ clusters, dark in (a) and bright in (b), respectively, decorating the faceted surface of a GaN nanowire. (c) X-ray spectrum of individual SnO₂ cluster acquired in the spot marked by the red cross (inset). (For interpretation of the references to color in this figure legend, the reader is referred to the web version of the article.)

The sensor was also tested for response towards possible interfering chemicals such as acetone and alkanes. The device shows relatively low response to hexane as compared to the alcohols while the response to acetone is similar to the device response to isobutanol. Fig. 7e shows a column graph of the percentage response of the device for each chemical. Percentage response R is defined as

$$R = \frac{(I_g - I_a)}{I_a} \times 100 \quad (1)$$

where I_g is the device current measured 300 s after the 40 sccm flow of analyte in breathing air is turned on. Similarly, I_a is the device current measured 300 s after the 40 sccm flow of breathing air is turned on.

4. Discussion

4.1. Photocurrent in GaN NWs

Most semiconductor surfaces possess electronic surface states and the impact of these surface states on electronic properties of the semiconductor have been described in [33]. Depending on the

nature of the surface states, they may carry positive or negative charge that is screened by the opposite charge inside the semiconductor material known as the space charge. Distribution of the space charge is related to the curvature of the valence and conduction bands in the space charge region by Poisson's equation. This surface band bending causes photo generated charge carrier separation when the light above the band gap energy is incident on the device. For a semiconductor with positive space charge region, holes move towards the surface whereas electrons have a tendency to remain in the bulk. This phenomenon is also observed in semiconducting nanowires where the formation of the depletion region occurs on the entire surface of the nanowire forming a central conducting region surrounded by a depletion region.

Photoconductive behavior of GaN nanowires has been discussed in [34,35]. As the diameter of the NWs used in this work is greater than 100 nm, we have a neutral conducting "core" in the center of the NWs and a depletion region at the surface. When a voltage is applied across the ends of the NW we observe the dark current of the device. In the presence of light an enhanced current is observed due to photo-generated charge carriers and their separation assisted by surface band bending. In our case, as the GaN

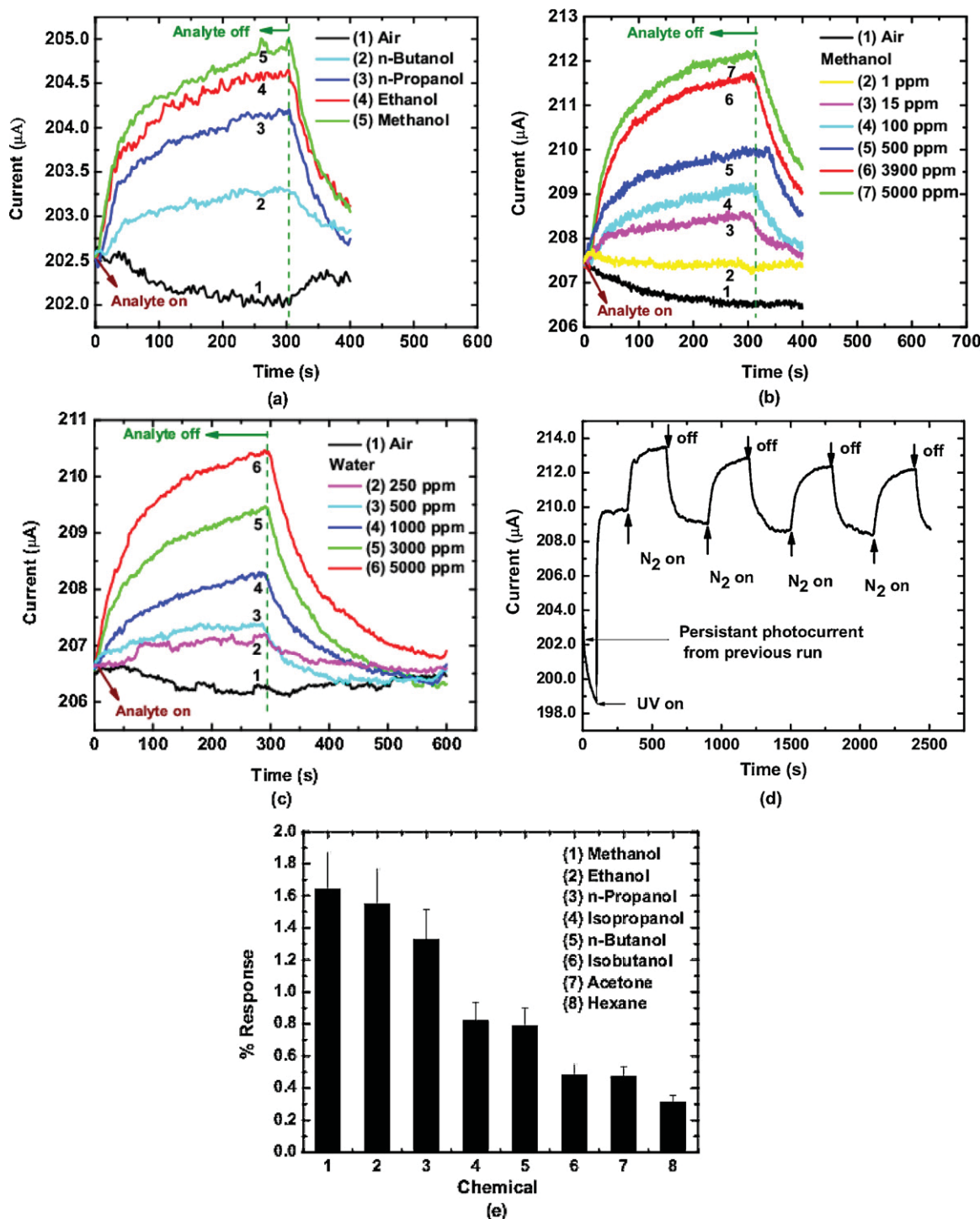


Fig. 7. Sensor response at room temperature in the presence of UV light to (a) alcohols at 500 $\mu\text{mol/mol}$ (ppm) concentration in air, (b) methanol from 1 $\mu\text{mol/mol}$ (ppm) to 5000 $\mu\text{mol/mol}$ (ppm) in air, (c) different humidity in air, (d) N_2 gas. (e) Response towards 500 $\mu\text{mol/mol}$ (ppm) of different analytes. Percentage response calculated as per Eq. (1). Standard deviation is based on the device response to 500 $\mu\text{mol/mol}$ (ppm) ethanol as measured on three different days over a period of 10 days.

nanowire surface is inert to chemical species, the photo-current remains unaltered when the chemical vapors are passed over the bare GaN nanowire devices.

4.2. Photoresponse of SnO_2/GaN hybrid nanostructure

The GaN nanowire surface in our sensor devices is coated with SnO_2 nanoclusters. SnO_2 , like most other semiconducting metal oxides, carries adsorbed oxygen on its surface and at room temperature it is most likely to exist as O_2^- species [36]. Oxygen

adsorbs on the surface capturing a negative charge from SnO_2 [$\text{O}_2(\text{g}) + \text{e}^- \rightarrow \text{O}_2^-(\text{ads.})$] and creates the surface depletion layer and upward band bending at the surface. Due to the closely matching band gap values of the two materials, photo generated electron hole pairs are produced both in the SnO_2 nanocrystals and the GaN nanowires. Photogenerated holes can remove the adsorbed oxygen from the oxide surface [$\text{h}^+ + \text{O}_2^-(\text{ads.}) \rightarrow \text{O}_2(\text{g})$] and release the captured electron back into the oxide as explained for metal oxide semiconductors [37] and also demonstrated for metal oxide NWs [38,39]. Therefore the adsorbed oxygen is released in the presence

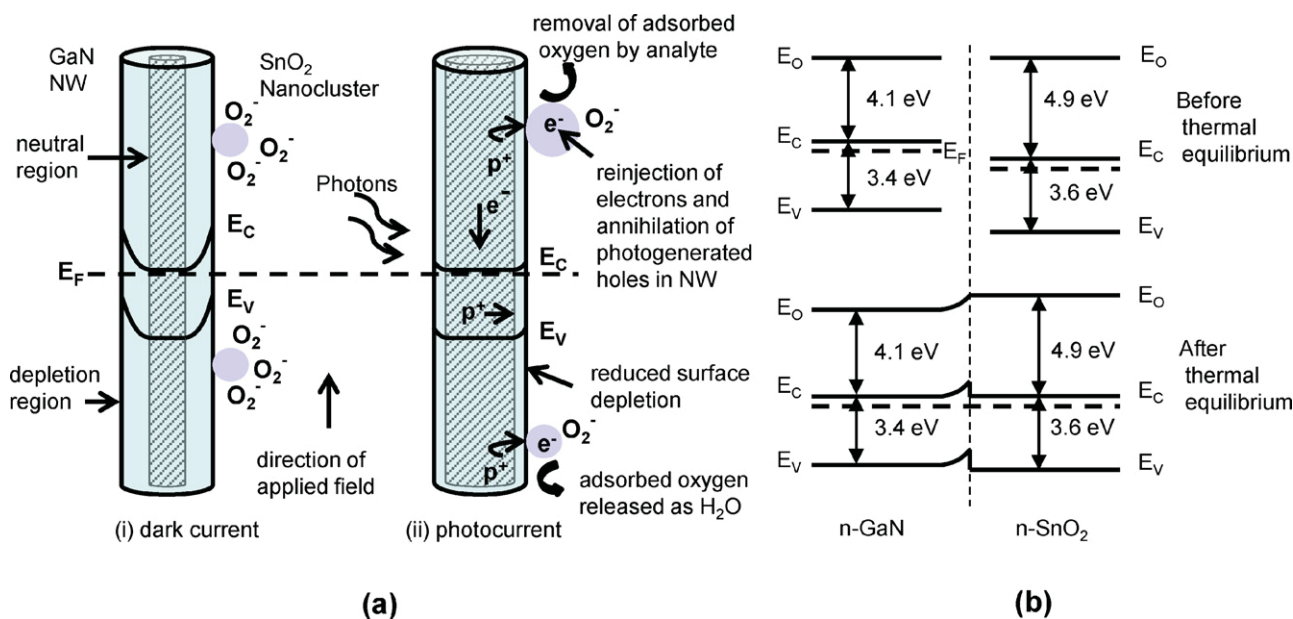


Fig. 8. (a) Schematic representation of sensing mechanism of SnO₂ coated GaN nanowire hybrid sensor. (b) Band diagram of SnO₂/GaN heterojunction.

of UV light and promotes photogenerated charge carrier separation in the SnO₂. The holes migrate towards the surface and the unpaired electrons are accumulated in the bulk of the nanocrystal. We speculate that these accumulated electrons promote photogenerated carrier separation in the GaN nanowire by trapping/recombining with the photogenerated holes in the NW at the surface. This leads to an increase in the device photocurrent.

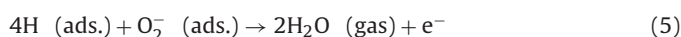
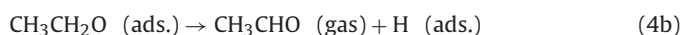
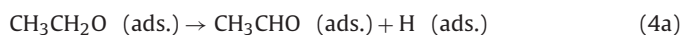
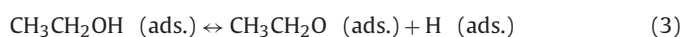
4.3. Sensor response to analytes

The proposed sensing mechanism explains the sensor response to the various chemical vapors tested in this work. Similar to the photogenerated holes, when chemical species interact with the adsorbed oxygen species, they may remove the O₂⁻ from the surface causing the captured electron to be released back into the SnO₂ [5]. Schematic representation of the proposed sensing mechanism has been shown in Fig. 8a. A qualitative band diagram of the GaN and SnO₂ semiconductor junction has been shown in Fig. 8b, where the impact of the nanoscale feature size of the SnO₂ nanoclusters on the material properties has not been considered.

4.3.1. Response to alcohols

The decomposition of alcohols on metal oxide surfaces in general, and SnO₂ in particular, has been widely studied. The adsorption and decomposition of alcohols on metal oxide surfaces could primarily proceed by (i) selective oxidation to aldehyde [5,11], (ii) dehydration to form alkene and water [11], and/or (iii) complete oxidation to carbon dioxide and water [40,41]. Selective oxidation to aldehyde seems to be the favored reaction on SnO₂ surface in the absence of catalytic additives. Thermal desorption spectroscopy of methanol on stoichiometric SnO₂ (1 1 0) surface detected formaldehyde and water as the only desorption products besides methanol [42].

A similar mechanism for dissociation of ethanol on the surface of single crystal and polycrystalline SnO₂ (1 1 0) to form acetaldehyde and water has been described in [11]. It has been suggested that gaseous ethanol can undergo a reversible dissociation to an ethoxy group and adsorbed hydrogen as



Although the above reactions have been shown to proceed only at temperatures above 300 K, the possibility is that UV excitation in our case promotes these reactions on the device surface even at room temperature [43]. Alternatively, alcohols could be dissociatively adsorbed as alkoxy group and hydrogen (step (3) above) without further dissociation to aldehyde at room temperature [44]. Through either route, hydrogen released in steps (3) or (4) can react with the adsorbed oxygen to form water and desorb from the oxide surface as shown in (5). This alcohol assisted removal of adsorbed oxygen to release free electrons in the oxide nanocrystals manifests itself as the increased conductivity in the nanowire in the presence of alcohol vapors.

When tested with various alcohol vapors, our devices show a response trend in the decreasing order of methanol > ethanol > n-propanol > isopropanol > n-butanol > isobutanol. This is opposite to the behavior observed with the SnO₂ thin films [45], other metal oxide nanostructures such as WO₃ nanoplates [46] and ZnO nanowires (our work, unpublished), i.e., the response is the highest for n-butanol and the lowest for methanol. The response trend of alcohols on thin films and nanowires can be explained by the fact that in gas phase the acidity of alcohols increases with the increasing length of the carbon chain in the molecule [47]. It has also been shown that the oxidation of alkoxy to aldehyde follows the same trend as the alcohols [44]. This implies that reactions (3) and (4) are the most favorable for butanol and butoxy respectively among all the alcohols under consideration. Therefore, we would expect to see highest response towards butanol and least towards methanol, as observed from metal oxide thin films and nanowires.

At present the reason for the reversal in trend from oxide thin film/nanowire to nanocrystalline coating is not understood, however we have confirmed our results by also fabricating ZnO NW sensors and comparing them with GaN NW sensor devices functionalized with ZnO nanocrystals (unpublished results). While the ZnO nanowire devices seem to follow the expected trend of decreasing response from butanol to methanol, we observe a

reverse trend in the GaN NW devices functionalized with ZnO nanocrystals.

4.3.2. Response to N_2 , H_2O and other analytes

When 40 sccm of nitrogen gas flow is introduced into the chamber in the absence of UV light, no change in the device current is seen. When the UV light is turned on, an increase in device current is recorded. In our understanding, nitrogen molecules displace adsorbed oxygen when supported by the photo generated holes. This is consistent with the results achieved with ZnO nanowire UV photodetectors where no change in dark current was observed in the vacuum before illumination, indicating that oxygen desorption was indeed supported by photogenerated holes [39].

Various possible mechanisms for interaction of water molecules with SnO_2 surface have been discussed [10]. An increase in surface conductivity in SnO_2 thin films in the presence of water has been experimentally proven [49]. The response of SnO_2 nanowires to H_2O at room temperature also shows an increase in conductivity when exposed to water vapors [50]. In our case, as with the SnO_2 nanowire, water should remove adsorbed oxygen on the surface, thus increasing the carrier separation in SnO_2 nanocluster and subsequently increasing the photocurrent in GaN NW. We do not exclude the possibility of ionic conductivity due to physisorbed water coating the surface of nanoparticles and nanowire [51]. However, electronic conductivity (replacement of adsorbed oxygen by water with release of electrons in the oxide) has been proposed as the major contributor to the humidity sensing mechanism of SnO_2 even at room temperature [52].

The sensor was also tested for response to acetone as it can be a common contaminant in alcohol vapors. The sensor response to acetone is low relative to methanol and ethanol but comparable to that for iso-butanol. A weaker response was observed to saturated alkanes such as hexane. The relative response of the sensor to various chemical vapors for a single device is summarized in Fig. 7e.

5. Conclusions

A hybrid (GaN nanowire)/(SnO_2 nanocrystals) sensor for selective alcohol sensing at room temperature has been fabricated. It has been shown that UV assisted sensing could be a substitute for temperature assisted metal oxide based sensing. We have shown that fairly inert GaN nanowires can be functionalized with active metal oxide nanocrystals to tune their response and selectivity to different classes of analytes. The SnO_2 functionalized GaN nanowire sensor selectively responds to first four organic alcohols (methanol, ethanol, propanol and butanol) and the isomers of propanol and butanol. The device shows a response and recovery time of the order of 100 s and has been tested for sensitivity between 1 $\mu\text{mol/mol}$ (ppm) and 5000 $\mu\text{mol/mol}$ (ppm). The suggested sensing mechanism utilizes oxidation of analyte molecules on the SnO_2 surface leading to increased photocurrent in GaN nanowire.

Acknowledgments

Research performed in part at the NIST Center for Nanoscale Science and Technology. VPO gratefully acknowledges the support from the NIST under contracts SB134110SE0579 and SB134111SE0814. Authors would like to thank Dr. Sergiy Krylyuk of NIST for useful inputs and comments.

References

- [1] S.R. Morrison, Semiconductor gas sensors, *Sensors and Actuators* 2 (1981) 329–341.

- [2] N. Barsan, D. Koziej, U. Weimar, Metal oxide-based gas sensor research: How to? *Sensors Actuators B: Chemistry* 121 (2007) 18–35.
- [3] X. Huang, Y. Choi, Chemical sensors based on nanostructured materials, *Sensors Actuators B: Chemistry* 122 (2007) 659–671.
- [4] A. Kolmakov, M. Moskovits, Chemical sensing and catalysis by one-dimensional metal-oxide nanostructures, *Annual Review of Materials Research* 34 (2004) 151–180.
- [5] M. Batzill, U. Diebold, The surface and materials science of tin oxide, *Progress in Surface Science* 79 (2005) 47–154.
- [6] A. Cabot, A. Diéguez, A. Romano-Rodríguez, J.R. Morante, N. Barsan, Influence of the catalytic introduction procedure on the nano- SnO_2 gas sensor performances: where and how stay the catalytic atoms, *Sensors Actuators B: Chemistry* 79 (2001) 98–106.
- [7] V. Dobrokhotov, D.N. McIlroy, M.G. Norton, A. Abuzir, W.J. Yeh, I. Stevenson, et al., Principles and mechanisms of gas sensing by GaN nanowires functionalized with gold nanoparticles, *Journal of Applied Physics* 99 (2006) 104302.
- [8] W. Lim, J.S. Wright, B.P. Gila, J.L. Johnson, A. Ural, T. Anderson, et al., Room temperature hydrogen detection using Pd-coated GaN nanowires, *Applied Physics Letters* 93 (2008) 072109–72113.
- [9] G.S. Aluri, A. Motayed, A.V. Davydov, V.P. Oleshko, K.A. Bertness, N.A. Sanford, et al., Highly selective GaN-nanowire/ TiO_2 -nanocluster hybrid sensors for detection of benzene and related environment pollutants, *Nanotechnology* 22 (2011) 295503.
- [10] N. Barsan, M. Schweizer-Berberich, W. Göpel, Fundamental and practical aspects in the design of nanoscaled SnO_2 gas sensors: a status report, *Fresenius' Journal of Analytical Chemistry* 365 (1999) 287–304.
- [11] D. Kohl, Surface processes in the detection of reducing gases with SnO_2 -based devices, *Sensors and Actuators* 18 (1989) 71–113.
- [12] G.F. Fine, L.M. Cavanagh, A. Afonja, R. Binions, Metal oxide semi-conductor gas sensors in environmental monitoring, *Sensors* 10 (2010) 5469–5502.
- [13] G. Sberveglieri, Classical and novel techniques for the preparation of SnO_2 thin-film gas sensors, *Sensors Actuators B: Chemistry* 6 (1992) 239–247.
- [14] E.R. Leite, I.T. Weber, E. Longo, J.A. Varela, A new method to control particle size and particle size distribution of SnO_2 nanoparticles for gas sensor applications, *Advanced Materials* 12 (2000) 965–968.
- [15] T.P. Hülser, H. Wiggers, F.E. Kruijs, A. Lorke, Nanostructured gas sensors and electrical characterization of deposited SnO_2 nanoparticles in ambient gas atmosphere, *Sensors Actuators B: Chemistry* 109 (2005) 13–18.
- [16] A. Kolmakov, Y. Zhang, G. Cheng, M. Moskovits, Detection of CO and O_2 using tin oxide nanowire sensors, *Advanced Materials* 15 (2003) 997–1000.
- [17] V.V. Sysoev, J. Goschnick, T. Schneider, E. Strelcov, A. Kolmakov, A gradient microarray electronic nose based on percolating SnO_2 nanowire sensing elements, *Nano Letters* 7 (2007) 3182–3188.
- [18] M. Law, H. Kind, B. Messer, F. Kim, P. Yang, Photochemical sensing of NO_2 with SnO_2 nanoribbon nanosensors at room temperature, *Angewandte Chemie International Edition* 41 (2002) 2405–2408.
- [19] S. Dmitriev, Y. Lilach, B. Button, M. Moskovits, A. Kolmakov, Nanoengineered chemiresistors: the interplay between electron transport and chemisorption properties of morphologically encoded SnO_2 nanowires, *Nanotechnology* 18 (2007) 055707.
- [20] Y. Lingmin, F. Xinhui, Q. Lijun, M. Lihe, Y. Wen, Dependence of morphologies for SnO_2 nanostructures on their sensing property, *Applied Surface Science* 257 (2011) 3140–3144.
- [21] S. Mathur, S. Barth, H. Shen, J. Pyun, U. Werner, Size-dependent photoconductance in SnO_2 nanowires, *Small* 1 (2005) 713–717.
- [22] J. Wu, C. Kuo, Ultraviolet photodetectors made from SnO_2 nanowires, *Thin Solid Films* 517 (2009) 3870–3873.
- [23] T. Oshima, T. Okuno, S. Fujita, UV-B sensor based on a SnO_2 thin film, *Japanese Journal of Applied Physics* 48 (2009) 120207.
- [24] A. Schleife, J.B. Varley, F. Fuchs, C. Rödl, F. Bechstedt, P. Rinke, et al., Tin dioxide from first principles: quasiparticle electronic states and optical properties, *Physical Review B* 83 (2011) 035116.
- [25] P. Feng, X.Y. Xue, Y.G. Liu, Q. Wan, T.H. Wang, Achieving fast oxygen response in individual $\beta\text{-Ga}_2\text{O}_3$ nanowires by ultraviolet illumination, *Applied Physics Letters* 89 (2006) 112114–112123.
- [26] L. Peng, T.F. Xie, M. Yang, P. Wang, D. Xu, S. Pang, et al., Light induced enhancing gas sensitivity of copper-doped zinc oxide at room temperature, *Sensors Actuators B: Chemistry* 131 (2008) 660–664.
- [27] T.Y. Yang, H.M. Lin, B.Y. Wei, C.Y. Wu, C.K. Lin, UV enhancement of the gas sensing properties of nano- TiO_2 , *Reviews on Advanced Materials Science* 4 (2003) 48–54.
- [28] B.P.J. de Lacy Costello, R.J. Ewen, N.M. Ratcliffe, M. Richards, Highly sensitive room temperature sensors based on the UV-LED activation of zinc oxide nanoparticles, *Sensors Actuators B: Chemistry* 134 (2008) 945–952.
- [29] K.A. Bertness, A. Roshko, L.M. Mansfield, T.E. Harvey, N.A. Sanford, Mechanism for spontaneous growth of GaN nanowires with molecular beam epitaxy, *Journal of Crystal Growth* 310 (2008) 3154–3158.
- [30] K.A. Bertness, A. Roshko, L.M. Mansfield, T.E. Harvey, N.A. Sanford, Nucleation conditions for catalyst-free GaN nanowires, *Journal of Crystal Growth* 300 (2007) 94–99.
- [31] A. Motayed, R. Bathe, M.C. Wood, O.S. Diouf, R.D. Vispute, S.N. Mohammad, Electrical, thermal, and microstructural characteristics of Ti/Al/Ti/Au multilayer Ohmic contacts to n-type GaN, *Journal of Applied Physics* 93 (2003) 1087–1094.
- [32] M. Batzill, W. Bergmayer, I. Tanaka, U. Diebold, Tuning the chemical functionality of a gas sensitive material: water adsorption on SnO_2 (1 0 1), *Surface Science* 600 (2006) 29–32.

- [33] H. Lüth, Surfaces and Interfaces of Solid Materials, 3rd ed., Springer, 1995.
- [34] N.A. Sanford, P.T. Blanchard, K.A. Bertness, L. Mansfield, J.B. Schlager, A.W. Sanders, et al., Steady-state and transient photoconductivity in *c*-axis GaN nanowires grown by nitrogen-plasma-assisted molecular beam epitaxy, *Journal of Applied Physics* 107 (2010) 034318–34414.
- [35] R. Calarco, M. Marso, T. Richter, A.I. Aykanat, R. Meijers, A.v.d. Hart, et al., Size-dependent photoconductivity in MBE-Grown GaN-Nanowires, *Nano Letters* 5 (2005) 981–984.
- [36] S. Chang, Oxygen chemisorption on tin oxide: correlation between electrical conductivity and EPR measurements, *Journal of Vacuum Science & Technology* 17 (1980) 366–374.
- [37] E. Comini, G. Faglia, G. Sberveglieri, Electrical-based gas sensing, in: E. Comini, G. Faglia, G. Sberveglieri (Eds.), *Solid State Gas Sensing*, Springer, US, 2009, pp. 1–61.
- [38] H. Kind, H. Yan, B. Messer, M. Law, P. Yang, Nanowire ultraviolet photodetectors and optical switches, *Advanced Materials* 14 (2002) 158–160.
- [39] C. Soci, A. Zhang, B. Xiang, S.A. Dayeh, D.P.R. Aplin, J. Park, et al., ZnO nanowire UV photodetectors with high internal gain, *Nano Letters* 7 (2007) 1003–1009.
- [40] T. Jinkawa, G. Sakai, J. Tamaki, N. Miura, N. Yamazoe, Relationship between ethanol gas sensitivity and surface catalytic property of tin oxide sensors modified with acidic or basic oxides, *Journal of Molecular Catalysis A: Chemical* 155 (2000) 193–200.
- [41] S. Park, H. Zheng, J.D. Mackenzie, Ethanol gas sensing properties of SnO₂-based thin-film sensors prepared by the sol-gel process, *Materials Letters* 17 (1993) 346–352.
- [42] V.A. Gercher, D.F. Cox, J. Themlin, Oxygen-vacancy-controlled chemistry on a metal oxide surface: methanol dissociation and oxidation on SnO₂ (1 1 0), *Surface Science* 306 (1994) 279–293.
- [43] J.D. Prades, R. Jiménez-Díaz, F. Hernandez-Ramirez, S. Barth, A. Cirera, A. Romano-Rodríguez, et al., Equivalence between thermal and room temperature UV light-modulated responses of gas sensors based on individual SnO₂ nanowires, *Sensors Actuators B: Chemistry* 140 (2009) 337–341.
- [44] M. Bowker, R.J. Madix, XPS, UPS and thermal desorption studies of alcohol adsorption on Cu (1 1 0): II. Higher alcohols, *Surface Science* 116 (1982) 549–572.
- [45] H. Gong, Y.J. Wang, S.C. Teo, L. Huang, Interaction between thin-film tin oxide gas sensor and five organic vapors, *Sensors Actuators B: Chemistry* 54 (1999) 232–235.
- [46] D. Chen, X. Hou, H. Wen, Y. Wang, H. Wang, X. Li, et al., The enhanced alcohol-sensing response of ultrathin WO₃ nanoplates, *Nanotechnology* 21 (2010) 035501.
- [47] J.I. Brauman, L.K. Blair, Gas-phase acidities of alcohols. Effects of alkyl groups, *Journal of the American Chemical Society* 90 (1968) 6561–6562.
- [49] V.E. Henrich, P.A. Cox, *The Surface Science of Metal Oxides*, Cambridge University Press, 1996.
- [50] Q. Kuang, C. Lao, Z.L. Wang, Z. Xie, L. Zheng, High-sensitivity humidity sensor based on a single SnO₂ nanowire, *Journal of the American Chemical Society* 129 (2007) 6070–6071.
- [51] T. Morimoto, M. Nagao, F. Tokuda, The relation between the amounts of chemisorbed and physisorbed water on metal oxides, *Journal of Physical Chemistry* 73 (1969) 243–248.
- [52] Z. Chen, C. Lu, Humidity sensors: a review of materials and mechanisms, *Sensor Letters* 3 (2005) 274–295.

Biographies

Ritu Bajpai received her B.Tech. degree in Electrical Engineering in 2006 from Institute of Technology, Banaras Hindu University at Varanasi, India. She is currently a Ph.D. degree candidate at The George Washington University, Washington, DC, USA. She has been working as a guest researcher in the Metallurgy Division, Material Metrology Laboratory (MML) at NIST since 2010. Her current research interests include fabrication and measurement of semiconducting nanowire electrical and optical devices for gas sensing.

Abhishek Motayed received his Ph.D. degree in 2007 from the Electrical and Computer Engineering department at the University of Maryland, College Park. During his graduate studies, he worked at the National Institute of Standards and Technology (NIST) as a guest scientist. Dr. Motayed continued working at NIST after graduating, with an appointment as a research scientist at the Institute of Research

in Electronics and Applied Physics at the University of Maryland. His current research expertise and interests are high-performance nanoscale electronic/optical devices with emphasis on large-scale integration, novel chemical/biological/radiation sensor systems, energy conversion/storage, and bio-medical applications of nanoscale devices.

Albert Davydov received the Ph.D. in Chemistry from Moscow State University (Russia) in 1989. He was an Assistant Professor of Chemistry at Moscow State University (1987–1993), an Invited Researcher at the University of Sheffield, UK (1992–1993), an Assistant Research Scientist at the University of Florida (1993–1997), and a NIST Research Associate at the University of Maryland (1997–2005). He joined NIST full-time in 2005 and is now active in the area of semiconducting nanowires/thin-film materials and devices. He is presently a Project Leader on “Semiconductor nanowires for sensorics, opto/electronics and energy applications” at the Metallurgy Division, Material Metrology Laboratory (MML/NIST).

Vladimir P. Oleshko earned Master’s degree in Physical Chemistry with high honors (1976) and a Ph.D. degree in Chemistry (1983) from Moscow State University, Moscow, Russia. Dr. Oleshko currently serves as a contract researcher at NIST for development of new analytical electron microscopy-based nanometrologies for emerging nanotechnology applications and as Adjunct Research Professor at The University of Arizona. He is coauthor of 4 inventions, 3 book chapters and 3 reviews and has published 71 refereed journal papers and more than 90 refereed conference papers.

Geetha S. Aluri received her B.Tech. degree in Electrical and Electronics Engineering in 2007 from GITAM University, Andhra Pradesh, India. She is currently a Ph.D. degree candidate at The George Mason University in Fairfax, VA, USA. She has been working as a guest researcher in the Metallurgy Division, Material Metrology Laboratory (MML) at NIST since Feb 2008. Her specializations and interests include fabrication and characterization of semiconducting micro and nanodevices, material processing technologies, and understanding fundamental transport properties in nanostructures.

Kris A. Bertness is a physicist in the Optoelectronics Division of the National Institute of Standards and Technology in Boulder, CO. Her technical focus has been on III–V semiconductor crystal growth, characterization, and device design, with particular emphasis on nanowires and quantum dots. NIST’s recent work GaN nanowires was recognized with an R&D Magazine MicroNano 25 Award in 2006. Prior to joining NIST in 1995, she developed record-efficiency solar cells with a team at the National Renewable Energy Laboratory. She received her Ph.D. in Physics from Stanford University.

Mulpuri V. Rao received the B.Tech. degree in electronics and communication engineering from the College of Engineering, Kakinada, India, in 1977, the M.Tech. degree in material science from the Indian Institute of Technology Bombay, Mumbai, India, in 1979, and the M.S. and Ph.D. degrees in electrical engineering from Oregon State University, Corvallis, in 1983 and 1985, respectively. From 1979 to 1981, he was a Lecturer in electronics and communication engineering at Sidhartha Engineering College, Vijayawada, India. Since August 1984, he has been with George Mason University, Fairfax, VA, where he is currently a Professor in the Electrical and Computer Engineering Department. He is the author or coauthor of more than 120 articles published in various journals in the areas of epitaxial growth, ion implantation, ohmic contacts, material characterization, photodetectors, microwave and high-power devices, microfluidic cells, gas sensing, etc.

Mona E. Zaghoul received the B.S. degree from Cairo University, Giza, Egypt, and the Master’s degree in science, the Master’s degree in math, and the Ph.D. degree from the University of Waterloo, Waterloo, ON, Canada, in 1965, 1970, 1971, and 1975, respectively. She is currently a Professor of electrical and computer engineering at the George Washington University (GWU), Washington, DC, where she is also Director for the Institute of MEMS and VLSI Technologies. She has published over 250 technical papers in the general areas of circuits and systems, microelectronics system design, VLSI circuits design, RF-MEMS, and microelectromechanical sensors systems. She has also contributed to several books. Since 1984, she has been with Semiconductor Devices Technology Division, the National Institutes of Standards and Technology, Gaithersburg, MD. Dr. Zaghoul received the 50th year Gold Jubilee Medal from the IEEE Circuits and Systems (CAS) Society in recognition of outstanding contributions to the society. She was the Vice President of IEEE-CAS Technical Activities in 1999–2001. She served as the President of the IEEE Sensors Council in 2008–2009.